

Supplement to “Investigation of the strength contrast at the Moho: A case study from the Oman Ophiolite”

Janelle M. Homburg, Greg Hirth, Peter B. Kelemen

1. Methods

1.1. Thin Section Preparation

Oriented thin sections were prepared from samples selected based on their texture and mineralogy. Samples analyzed by EBSD were polished for an additional hour on 0.02 μm colloidal silica beyond the polishing done for microprobe analysis. Microprobe samples were C coated. EBSD samples were Au-Pd coated and then polished for an additional minute to remove most of the coating, leaving enough gold along cracks and grain boundaries to mitigate sample charging in the SEM.

1.2. Grain Size Analysis

Mean grain size was measured by line intercept method for plagioclase in the gabbro norite and olivine in the harzburgite. At least 100 grains were measured parallel to foliation. Because the grains are roughly equant, a geometric correction factor of 1.5 has been applied to the mean intercept lengths to obtain the average grain size (Underwood, 1970). The arithmetic mean was calculated to be consistent with Van der Wal (1993). However, since the grain size distributions are approximately log-normal, the geometric mean may be a more accurate measure of the average grain size. Both are given in Figure DR3.

1.3. Thermometry

1.3.1. Pyroxene Thermometry

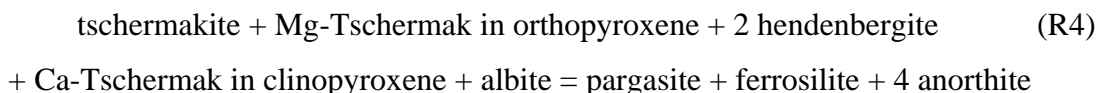
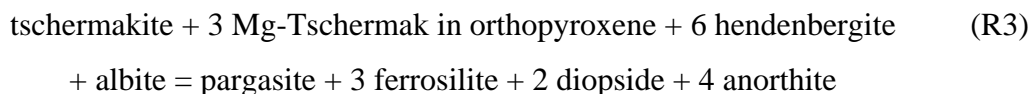
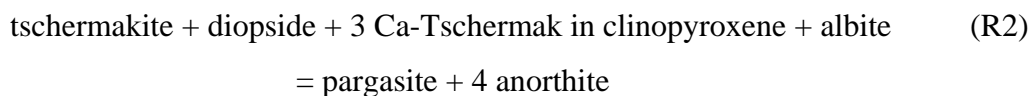
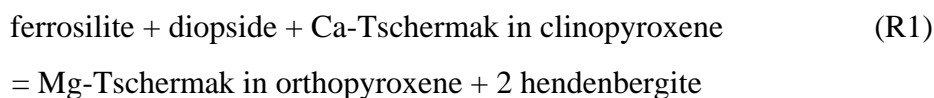
Equilibrium temperatures were calculated for clinopyroxene/orthopyroxene pairs in the recrystallized rims of clinopyroxene porphyroclasts. The measured grains are equant with an average grain size of 220 μm . Oxide weight percents were measured using the JEOL JXA-733 Superprobe (Massachusetts Institute of Technology), with a 10 μm spot size, 10 nA beam current and an accelerating voltage of 15 kV (Table DR1). Using Ca-QUILF (Andersen et al., 1993; Lindsley and Frost, 1992), temperatures were calculated for 6 clinopyroxene/orthopyroxene pairs (Table DR1).

1.3.2. Amphibole/Plagioclase Thermometry

Equilibrium temperatures were calculated for metamorphic amphibole/plagioclase pairs in the tails of recrystallized clinopyroxene porphyroclasts. Average grain size of the measured amphibole is 175 μm along the long axis of the grains and 70 μm along the short axis, yielding an aspect ratio of 2.5. Oxide weight percents were measured using the Cameca Sx100 microprobe (The American Museum of Natural History), with a 10 μm spot size, 10 nA beam current and an accelerating voltage of 15 kV (Table DR3). Temperatures were calculated for 4 amphibole/plagioclase pairs using HB-PLAG (Holland and Blundy, 1994, reaction A). (Plagioclase composition is roughly constant in every sample that was measured.) A range of temperatures of 600-800°C was calculated for the observed amphibole and plagioclase compositions (Tables DR2 and DR3). The average temperature calculated is 700°C. The standard deviation of the calculated temperatures is 80°C. However, reaction A involves quartz, whereas there is no quartz in our samples. As a result, the temperatures for Reaction A, derived from our amphibole compositions, represent upper bounds for the reaction at reduced silica activity.

1.3.4 THERMOCALC

Using the “mode 3” method of THERMOCALC (Powell and Holland, 1988) we determined equilibria for reactions based on the activities of mineral end-members for our plagioclase, pyroxene and most sodic amphibole compositions. We used four reactions to constrain temperature and pressure:



Based on these reactions we calculated equilibrium pressures and temperatures of 550 ± 300 MPa and $570\pm 200^{\circ}\text{C}$ for the feldspar 8 from Table DR2, the pyroxene “Pair 5” from Table DR1 and the amphiboles 1 and 3 from Table DR3 (Figure DR4).

1.4. EBSD Analysis

EBSD data were collected using a JEOL 840 SEM (Marine Biological Laboratory/Woods Hole Oceanographic Institution) at 15 kV and a beam current of 6×10^{-8} amps. Both the olivine and plagioclase data were analyzed utilizing the HKL Channel 5+ software. The olivine data were collected by manual selection of the diffraction patterns. The plagioclase data were collected as maps with a step size of $15 \mu\text{m}$ (approximately the grain size) to insure sufficient spatial coverage of the areas of interest. For each area of interest, >150 grain orientations were obtained. This number has been shown to be sufficient to allow for robust comparisons of both fabric pattern and strength (Ben Ismail and Mainprice, 1998).

2.1 Plagioclase Microstructures

All of the gabbro-norite samples display evidence of plastic deformation. In the least deformed samples we observe the development of porphyroclasts ($\sim 500 \mu\text{m}$), which display extensive deformation twinning and subgrain development, rimmed by small recrystallized grains ($\sim 40 \mu\text{m}$) (Figure DR5). In the most deformed samples we observe mylonitic textures. The grains in the mylonites display no subgrain development, little twinning and curved, irregular boundaries (Figure 2A). In none of the samples do we observe evidence that melt was present during deformation and have interpreted the porphyroclastic grain size in the least deformed samples as representing the original igneous grain size of the plagioclase. Finally, because large portions of the fine grained ($40 \mu\text{m}$) regions display an LPO, which reflects activity of dislocation creep, it seems unlikely that they represent annealed fault gouge rather than mylonites. Furthermore, the observation that the entire thickness of the deformed dikes shows evidence for crystal plastic deformation, while only the highest strain zone show complete recrystallization argues against a brittle precursor, although it would be difficult to rule this out.

2.2. Zener Pining Analysis

To explore the possibility that grain growth subsequent to deformation can affect the observed grain size we used a Zener pinning relationship with the form:

$$d = k \frac{d_{pin}}{f^m} \quad (1)$$

where d is the matrix grain size, d_{pin} is the pinning phase grain size, f is the volume fraction of the pinning phase, k is a proportionality constant and m depends on grain topology (e.g. Olgaard and Evans, 1986) to calculate the predicted pinned plagioclase grain size where amphibole is present. Using $k = 1.45$ and $m = 0.34$ (Mehl and Hirth (2008)), the average predicted plagioclase grain size is 30 μm for an area with an average observed plagioclase grain size of 14 μm . This suggests that neither annealing nor secondary phase pinning significantly affected the plagioclase grain size and that the observed grain size reflects the recrystallized grain size during deformation. Annealing may have been mitigated by the rapid cooling of these oceanic rocks (e.g., Mehl and Hirth, 2008).

References

- Andersen, D.J., Lindsley, D.H., and Davidson, P.M., 1993, QUILF: A Pascal program to assess equilibria among Fe-Mg-Mn-Ti oxides, pyroxenes, olivine and quartz: *Computers & Geosciences*, v. 19, p. 1333-1350.
- Ben Ismaïl, W., and Mainprice, D., 1998, An olivine fabric database: and overview of upper mantle fabrics and seismic anisotropy: *Tectonophysics*, v. 296, p. 145-157.
- Holland, T.J.B., and Blundy, J., 1994, Non-ideal interactions in calcic amphiboles and their bearing on amphibole-plagioclase thermometry: *Contributions to Mineralogy and Petrology*, v. 116, p. 433-447.
- Lindsley, D.H., and Frost, B.R., 1992, Equilibria among Fe-Ti oxides, pyroxenes, olivine, and quartz: Part I. Theory: *American Mineralogist*, v. 77, p. 987-1003.
- Mehl, L., and Hirth, G., 2008, Plagioclase preferred orientation in layered mylonites: Evaluation of flow laws for the lower crust: *Journal of Geophysical Research*, v. 113, p. doi:10.1029/2007JB005075.
- Nicolas, A., and Boudier, F., 2008, Large shear zones with no relative displacement: *Terra Nova*, v. 20, p. 200-205.
- Olgaard, D.L., and Evans, B.W., 1986, Effect of second-phase particles on grain growth in calcite: *Journal of the American Ceramic Society*, v. 69, p. C-272 - C-277, doi:10.1111/j.1151-2916.1986.tb07374.x.
- Powell, R., and Holland, T.J.B., 1988, An internally consistent dataset with examples and a computer program: *Journal of Metamorphic Geology*, v. 6, p. 173-204.
- Underwood, E.E., 1970, *Quantitative Stereology*, 274 pp., Addison-Wesley-Longman, Reading, Mass.
- Van der Wal, D., 1993, Deformation processes in mantle peridotites. Ph.D. thesis, Utrecht, *Geologica Ultraiectina* 102.

Figures

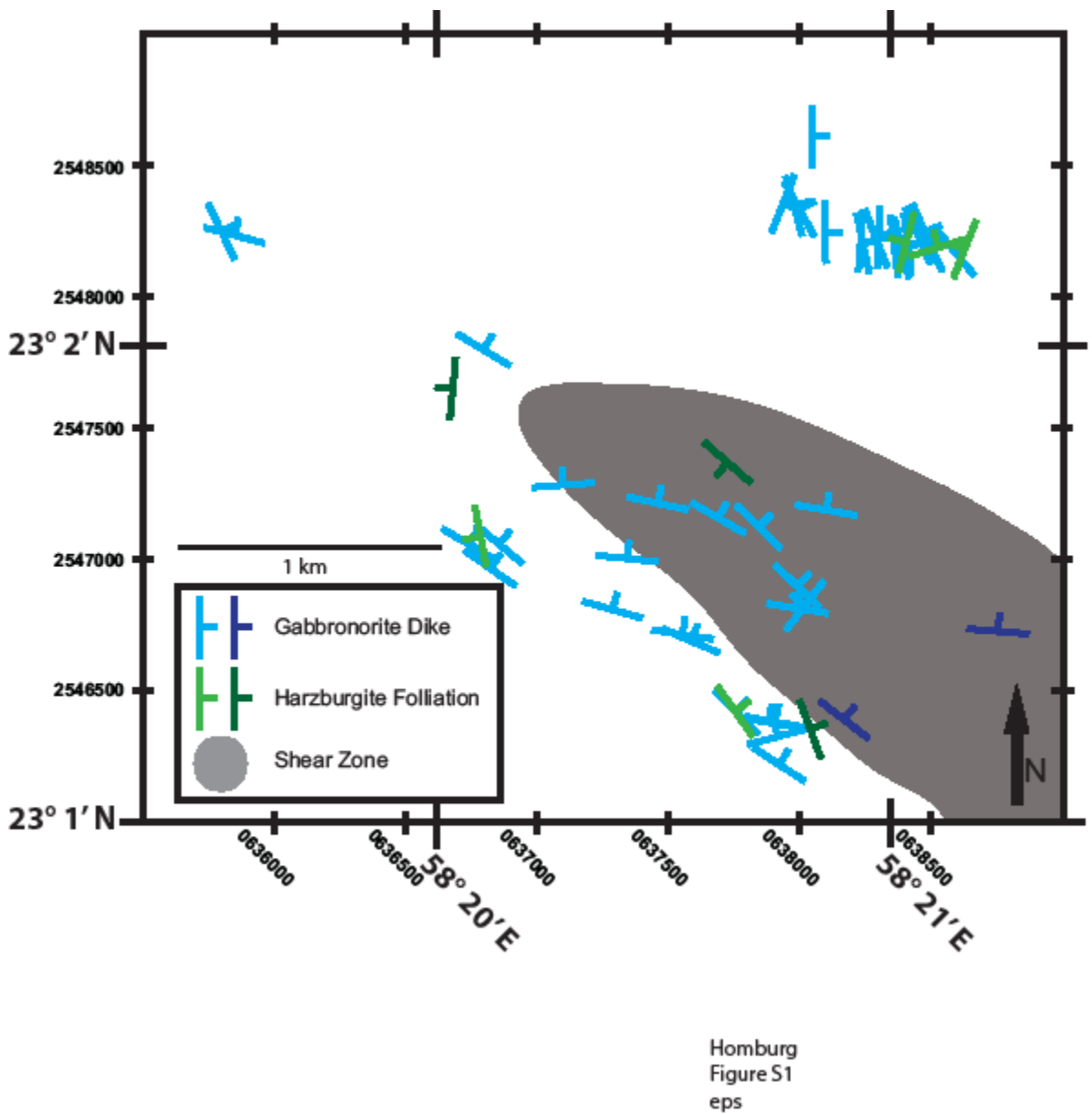
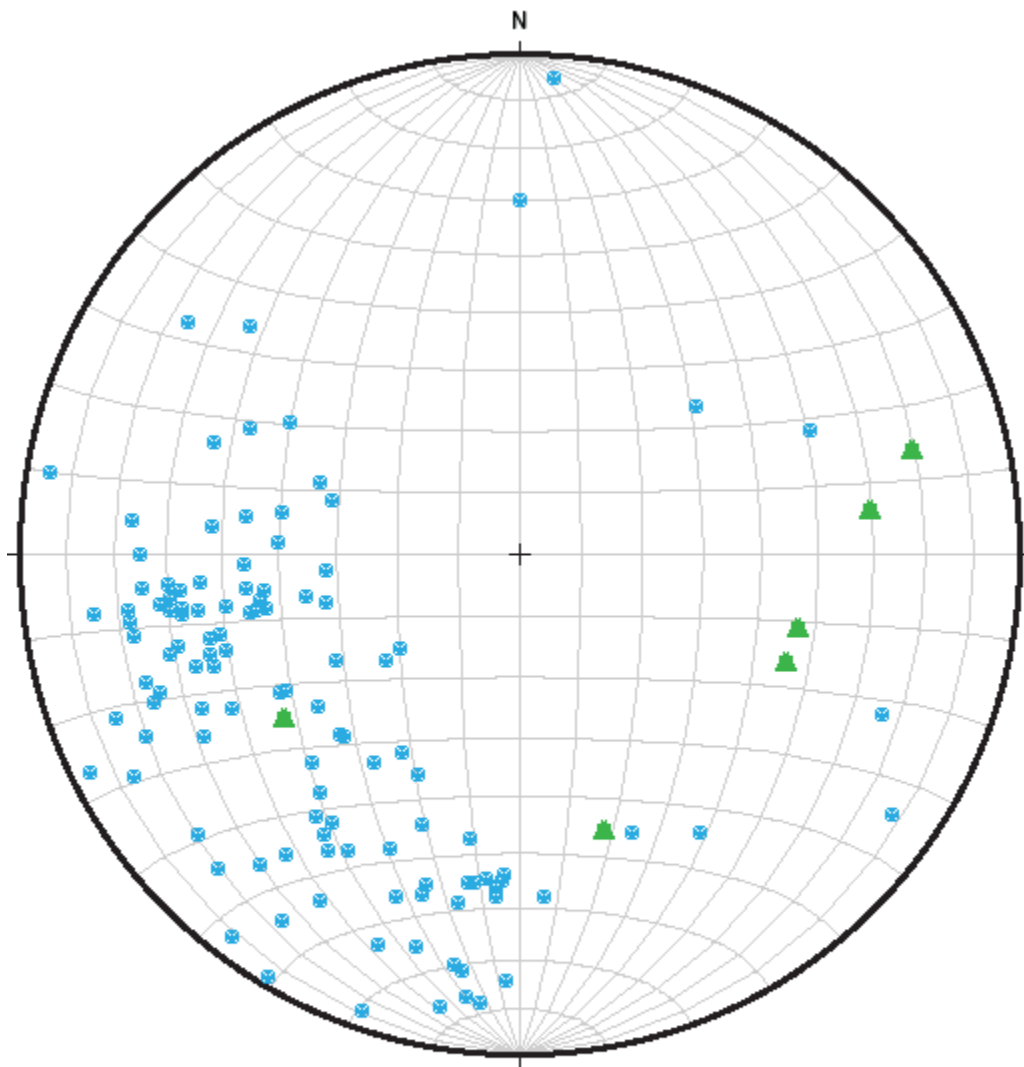
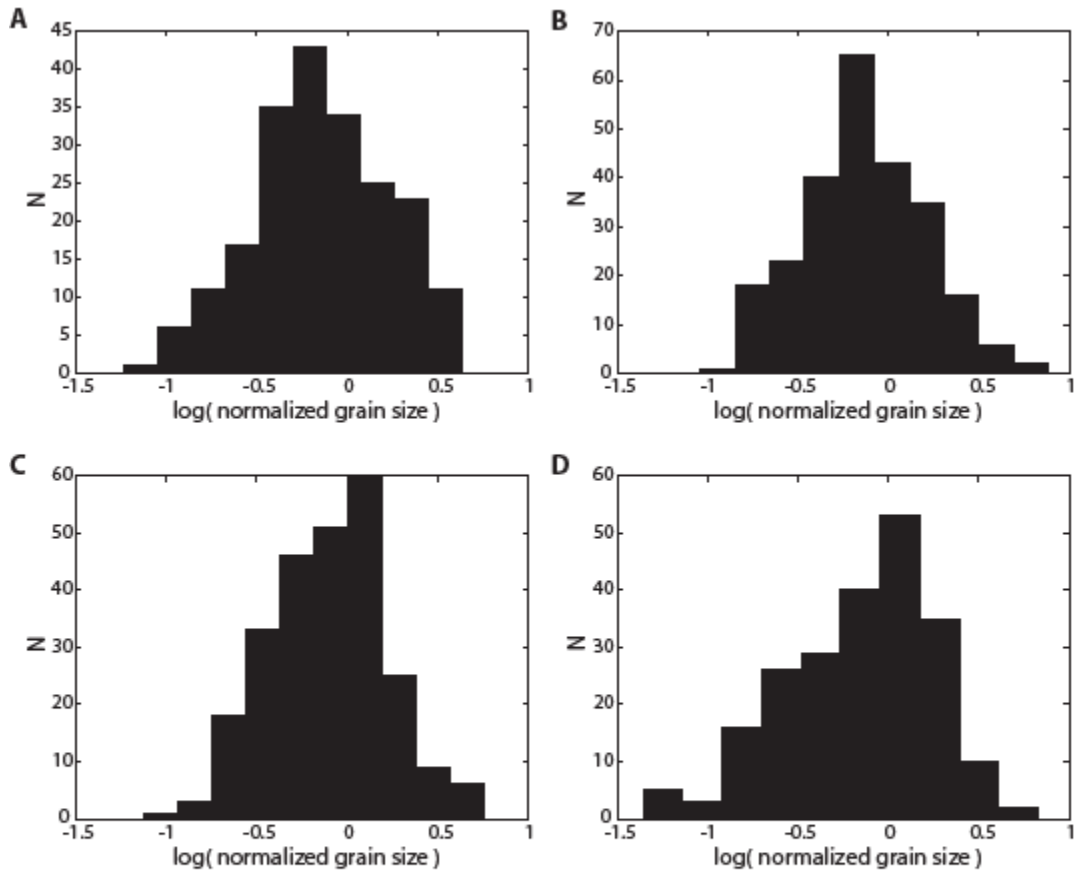


Figure DR1: Map of the field area containing orientation measurements of gabbro dike (blue) and harzburgite foliation (green). The darker colors represent measurements taken from Nicolas and Boudier (2008). The grey field is the trace of the mantle shear zone identified by Nicolas and Boudier (2008).



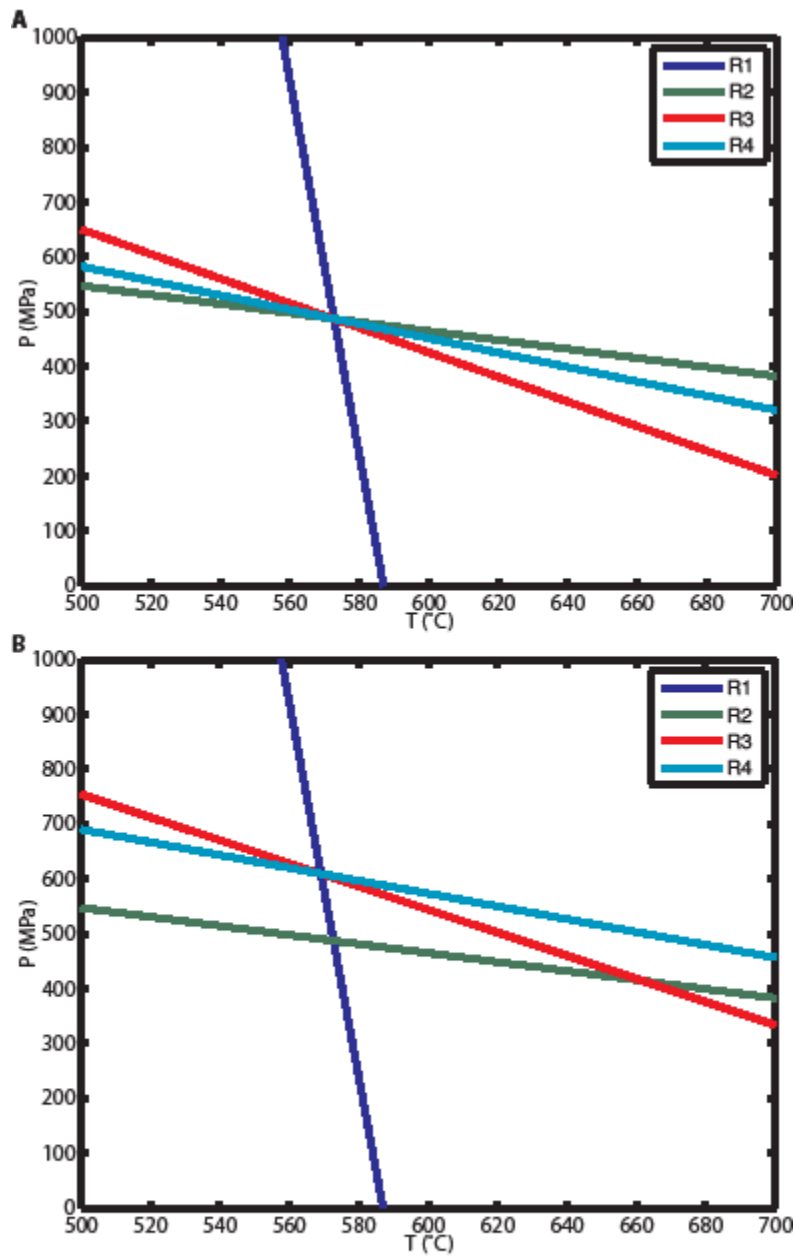
Homburg
Figure S2
eps

Figure DR2: Equal area projection of gabbro dike orientation (blue) and harzburgite foliation (green).



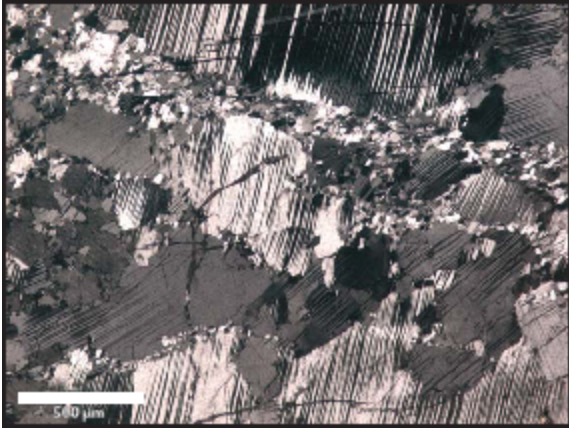
Homburg
Figure S3
eps

Figure DR3: Grain size distributions that correspond to A-C) the plagioclase in the three areas of the gabbro mylonite shown in Figure 2A 1-3) and D) the olivine in the harzburgite shown in Figure 2B. N is the number of grains. The standard deviations of grain size for plagioclase range from 33-73% of the mean with the largest standard deviations corresponding to areas that display disequilibrium deformation textures. The standard deviations of the grain size range from 58-76% of the mean for olivine.



Homburg
Figure S4
eps

Figure DR4: Equilibria calculated for amphiboles A) 1 and B) 3. R1 – R4 refer to R1 – R4 in text.



Homburg
Figure S5
eps

Figure DR5: Photomicrograph of a relatively undeformed gabbro-norite dike displaying highly twinned porphyroclasts rimmed by small recrystallized grains.

Table DR1: Pyroxene pair compositions given in oxide percent and estimated temperatures.

Pair	Phase	SiO ₂	TiO ₂	Al ₂ O ₃	Cr ₂ O ₃	FeO	MnO	MgO	CaO	Na ₂ O	Total	Temperature (°C)
1	OPX	54.93	0.0673	1.741	0.0248	11.68	0.2657	30.33	0.5498	0.0139	99.6	827 ± 46
	CPX	52.81	0.1591	1.9191	0.0702	3.83	0.0915	16.51	23.88	0.0857	99.36	
2	OPX	54.81	0.0436	1.6996	0.0192	11.59	0.2658	29.94	0.5052	0	98.87	821 ± 59
	CPX	52.68	0.1673	1.8833	0.0581	4.02	0.1483	16.53	23.77	0.0573	99.32	
3	OPX	54.37	0.0428	1.3612	0.0202	12.47	0.2533	29.62	0.4056	0.014	98.56	828 ± 152
	CPX	53.13	0.1271	1.6323	0.0421	4.24	0.165	16.61	23.71	0.0372	99.69	
4	OPX	54.65	0.0652	1.5831	0.056	12.74	0.2984	29.16	0.4889	0	99.04	804 ± 17
	CPX	52.96	0.1764	1.6703	0.0308	3.99	0.1176	16.33	23.72	0.04	99.04	
5	OPX	54.28	0.0376	1.6951	0.0218	12.82	0.1905	29.11	0.6351	0	98.79	854 ± 73
	CPX	52.45	0.1552	2.58	0.031	4.48	0.1224	16.07	24.1	0.0418	100.02	
6	OPX	54.48	0.0508	1.4592	0.0115	14.16	0.2563	28.38	0.4401	0	99.24	759 ± 66
	CPX	53.02	0.1383	1.4153	0.0216	4.18	0.0885	16.28	24.52	0.0071	99.66	

Table DR2: Plagioclase compositions given in oxide percent.

Analysis	SiO ₂	Al ₂ O ₃	FeO	MgO	CaO	Na ₂ O	K ₂ O	Total	An Content
1	44.42	36.61	0.1373	0.0113	19.94	0.2096	0.003	101.34	98
2	44.31	36.4	0.1023	0.0094	19.79	0.2694	0.003	100.88	98
3	43.96	36.53	0.0688	0.0065	19.72	0.2219	0	100.52	98
4	43.88	36.41	0.077	0.0026	19.66	0.3195	0.0024	100.35	97
5	44.45	35.61	0.1598	0.0155	19.76	0.2548	0	100.25	98
6	44.39	36.38	0.1024	0.0132	19.53	0.306	0.0079	100.73	97
7	44.04	36.23	0.0854	0.0169	20.04	0.2463	0.0103	100.67	98
8	43.22334	36.48335	0.02464	0.0064	20.03069	0.17568	0.02153	100	98
9	43.0015	36.48624	0.11426	0.00715	20.1656	0.10691	0.00418	99.96786	99
10	43.06566	36.34677	0.08497	0.00638	20.03998	0.19592	0.01607	99.75961	98
11	43.44502	36.28052	0.04823	0	19.73167	0.30101	0	99.84606	97
12	43.4904	36.36016	0.03253	0	19.88632	0.16132	0.01132	100.0355	98
13	42.8625	36.18185	0.08807	0	19.94982	0.31141	0.0089	99.44111	97

Analyses measured using a JEOL JXA-733 Superprobe (Massachusetts Institute of Technology)
Analyses measured using a Cameca Sx100 microprobe (The American Museum of Natural History)

Table S3: Amphibole compositions given in oxide percent

Analysis	SiO ₂	TiO ₂	Al ₂ O ₃	Cr ₂ O ₃	FeO	MnO	MgO	CaO	Na ₂ O	K ₂ O	Total	MG #
1	52.05265	0.28234	5.23215	0.0182	8.58851	0.16026	17.94999	12.17576	0.63172	0.12982	97.22141	79
2	53.65453	0.04115	3.12762	0	14.10423	0.57421	19.80348	6.07873	0.41733	0.02205	97.82333	71
3	54.57003	0.11003	2.52649	0.016	11.27614	0.35703	20.25484	8.16851	0.35962	0.01891	97.65759	76
4	54.88121	0.07997	2.02167	0	13.99136	0.60809	20.95897	4.61728	0.28469	0.02001	97.46325	73
5	55.70098	0.00926	1.52679	0.01681	10.60965	0.39185	20.66375	8.55836	0.20571	0.00726	97.69041	78